Modeling Non-Linearities of Power Electronic Converters Using Artificial Neural Networks

Andrea Zilio, Davide Biadene, Tommaso Caldognetto and Paolo Mattavelli
Department of Management and Engineering
University of Padua, Vicenza, Italy
Email: andrea.zilio.5@phd.unipd.it, davide.biadene@unipd.it, tommaso.caldognetto@unipd.it, paolo.mattavelli@unipd.it

***Abstract*—An approach based on Artificial Neural Networks (ANNs) for the average modeling non-linearities in power electronic converters is explored in this paper. The aim is to analyze the effectiveness of non-linear autoregressive exogenous NARX-ANN to realize an average black-box dynamic model of dc-dc converters that includes converter non-linearities in time and frequency domains within the same framework. The effectiveness of the proposed solution is evaluated by means of simulation and experimental results on a boost converter as test-case. The validity of the model is verified by comparing the time responses and transfer functions at different operating points, focusing on the non-linearities caused by the coexistence between the discontinuous conduction mode (DCM) and the continuous conduction mode (CCM) in the same model.**

***Index Terms*—Artificial Neural Network (ANN), modeling power converter, discontinuous conduction mode (DCM), continuous conduction mode (CCM)**

I. Introduction

Recently, broad interest is growing in the application of artificial intelligence (AI) in numerous scientific and industrial fields. Power electronic conversion circuits, and powerful digital controllers, present many compelling scenarios in which AI methods may unleash unprecedented performances, new features, and potential breakthrough applications [1].

An electronic power system, such as a smartgrid, commonly comprises a large number of electronic power converters (EPCs) from different manufacturers. Hence, owing to their confidentiality, a system designer has no access to detailed data about the internal structure of the converters, weakening the stability assessment and critical fault responce of the whole system. Therefore, conventional structural models based on knowledge of power converter parameters may not be used [2]. To overcomes these issues, it is necessary to estimate the static and dynamic performance of the EPC either by directly identifying its parameters or by determining an equivalent structure that can emulates its behavior [3].

In literature, several approaches are available for power converters modeling [4]. White-box models are derived by applying first principles of physics, they accurately explain the architecture of the system and provide a clear physical interpretation of it. Switching models fall within this category. Grey-box methods, however, are used when only a part of the system architecture is known, for example the reduced-order average models. These two methods have a common drawback, they require some prior knowledge about the system that is not always available.

Black-box modeling are model-free approaches that can potentially overcome these limits. Black-box model parameters have no physical meaning, they are only a means of matching input-output relationships. Input-output experiments can therefore be used as the principal source of data for these type of data-driven approach.

In the literature, black-box analytical methods are classified according to the type of response that they are able to reproduce. The structure of these methods is divided into three categories: linear, static non-linear and dynamic non-linear [5]. In the linear approach, models are built to replicate the small-signal behavior of the EPC at a specific operating point [6].

In the static non-linear structures the Wiener-Hammerstein approach is the most common method and it is the most widely used. In this approach, the dynamic behavior of the system is described using a passive network (i.e., consisting of passive components like capacitors, inductors or resistors), while the non-linear behavior is described using voltage or current sources controlled by non-linear functions [7], [8]. The main drawback is the linear dependency between the complexity of the system to be modeled (e.g., the number of poles and zeros) and the network modeling the non-linear behavior.

In dynamic non-linear methods the polytopic functions [5] are widely used. This approach describes the behavior of non-linear systems by obtaining small-signal models at different operating points and integrating them into a non-linear structure using weighting functions [9]. In order to achieve an accurate model of the EPC even in non-linearity, it is necessary to define a large number of transfer functions. However, this could lead to an increase in the complexity of the obtained model.

Some approaches based on the use of AI are already present in literature. In [10] a NARX-ANN is used for modeling a synchronous boost converter in CCM without experimental validation. A synchronous boost converter that operates in CCM is modeled in [11] and [12] in time domain only, while the frequency response accuracy is not addressed. An approach for modeling both the DCM and CCM operating modes of a converter using long short-term memory (LSTM) networks is presented in [13], however the frequency response matching is not investigated. In addition the LSTM-ANN, compared to

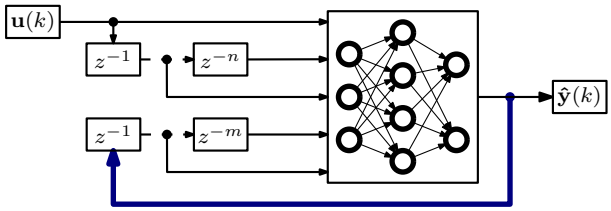

(a)

Fig. 1: Closed-loop configurations of NARX-ANN model.

the NARX-ANN, has a more complex structure that brings a higher number of parameters [14].

This paper is meant to be a preliminary investigation of ANN-based modeling applied to EPC characterization. To this end, the average small-signal model of a boost converter is proposed using NARX-ANN able to precisely replicate the converter dynamic behavior under different operating points. NARX-ANN to model CCM operation has already been applied with good results, while similar results are not reported considering DCM operation. Moreover, this article aims to demonstrate how it is possible to use NARX-ANN not exclusively to replicate the behavior in time domain but also to determine the small-signal transfer functions in DCM and CCM.

Section II provides several theoretical concepts about the NARX-ANNs and the reasons why they are used to achieve the aim describes in this paper. Section III outlines the boost converter used as test-case and shows the performance of the NARX-ANN using simulation data. Furthermore, information about the architecture of the ANN and indications on how the dataset is designed are provided. While, Section IV describes the experimental setup used for training the NARX-ANN and verifies the effectiveness of the proposed solution in time and frequency domains. Conclusions are reported in section VI.

II. Basics of NARX-ANN

To take into account the dynamic behavior of an EPC, an ANN with a memory effect should be considered by analogy with a state-space representation of the system. Among different types of recursive neural networks (RNNs) used for time series prediction [15], a NARX-ANN has been adopted in this work. NARX-ANN models can be used to model a wide variety of non-linear dynamic systems and they have been applied in various applications including time-series modeling [16]. Unlike other types of RNN, such as LSTM-ANN, in which the memory effect is implemented directly inside the neurons (i.e., the atomic computing units of ANN), the NARX-ANN are composed by two blocks as depicted in Fig. 1. A multilayer perceptron artificial neural network (MLP-ANN) is used to map the correlations between inputs and outputs, while an external delayed feedback is used to delay outputs and pass them as input to the ANN. The combination of the two blocks replicates the meaning of a state function.

ANN-NARX models have two different architectures, namely, the open-loop and the closed-loop architecture (Fig. 1), also known as series-parallel and parallel architecture, respectively.

The system equation describing the behavior of the NARX-ANN in open-loop operation is

$$\hat{\mathbf{y}}(k) = F\left[\,\mathbf{u}(k), ..., \mathbf{u}(k-n), \mathbf{y}(k-1), ..., \mathbf{y}(k-m)\,\right] \quad (1)$$

where $\hat{\mathbf{y}}(k)$ is the predicted vector of the outputs at the k-th instant, $\mathbf{u}(\cdot)$ and $\mathbf{y}(\cdot)$ are the input and output vectors of the system respectively, and $F(\cdot)$ is the non-linear function of MLP-ANN. The observation window of input and output vectors is defined by n and m values that represent the numbers of introduced delays in the NARX-ANN structure. The system equation describing the behavior of the NARX-ANN in closed-loop operation is

$$\hat{\mathbf{y}}(k) = F\left[\,\mathbf{u}(k), ..., \mathbf{u}(k-n), \hat{\mathbf{y}}(k-1), ..., \hat{\mathbf{y}}(k-m)\,\right] \quad (2)$$

where the predicted output $\hat{\mathbf{y}}(k)$ is a function of the input vector $\mathbf{u}(\cdot)$ and its own predicted outputs $\hat{\mathbf{y}}$ ignoring the previous outputs of the system $\mathbf{y}(\cdot)$.

The non-linear mapping function $F(\cdot)$ is initially unknown and it is approximated during the training process.

In the proposed approach herein, the series-parallel architecture is used during the training processes, and the error obtained from the comparison between the true value and that estimated one is used to update the network weights. Once the ANN is trained, it is converted into the closed-loop architecture to allow multi-step ahead prediction.

The basic elements in an MLP-ANN are *i*) number of layers, *ii*) number of neurons in each layer, *iii*) activation function of each layer, *iv*) algorithm used during training process [17].

In MLP-ANNs there are at least three layers: the input, the output and the shallow layer. The internal layers between input and output are denoted as hidden layers. Commonly, the higher the problem's complexity (i.e., the complexity of the function to be estimated), the higher the number of neurons and hidden layers required. Unfortunately, it is not possible to theoretically determine *a-priori* how many hidden layers or neurons are needed for a given problem.

The output of a neuron is defined as a linear combination of the inputs, and the resulting output is passed to a non-linear function called activation function. The ability of an ANN to be used for the analysis of non-linear problems is given by the use of activation functions that are not linear. Among different types of activation functions [18], in this work the Sigmoid activation function is used for the hidden layers while the ReLU one for the output layer.

III. Test case: Boost Converter

To demonstrate the effectiveness of the NARX-ANN in modeling non-linearities of an EPC, a boost converter is considered as case study. DCM and CCM operations are characterized in such a converter by two transfer functions with different poles and zeroes, which is evidence of the non-linear nature of the converter operation [19].

The theoretical model of the boost converter is shown in Fig. 2 and its parameters are reported in Tab. I.

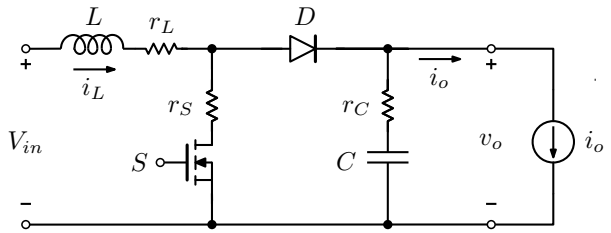

Fig. 2: Model of the boost converter.

TABLE I: Boost converter parameters.

Parameter	Symbol	Value	
Switching frequency	f_{sw}	20	kHz
Input Voltage	V_{in}	150	V
Inductance	L	340	µH
Capacitance	C	5.7	µF
Inductance Resistance	r_L	500	mΩ
Capacitance Resistance	r_S	100	mΩ
Switching Resistance	r_S	50	mΩ
Duty Cycle	δ	10-30	%
Output Current	i_o	0.8-3	A

A. Dataset Definition

To address the problem analyzed in this paper, the dataset characteristics must be designed to include information on both static and dynamic operations at different operating conditions.

For linear system, the AC sweep test is the typical and most applied system identification method in power electronics. For example, a method to measure the loop-gain frequency response experimentally through an AC sweep test is presented in [20]. In [21], the small-signal frequency response is obtained by applying Fourier analysis on the impulse response using a pseudo-random binary signal as approximation of white noise. Using this method, the required time for characterization is drastically reduced in comparison to the conventional AC sweep. While, [22] proposed a multi-sine excitation in combination with Fourier analysis for fast characterization of the control-to-output frequency response.

Nevertheless, EPCs are non-linear systems as the relationships between input and output variables, in general, depend on the operating point. When the model is aimed to describe the converter over its whole operating range, it is necessary to consider that small-signal analysis is not sufficient since it describes the behavior only locally. Therefore, previous approaches are in general valid for linear or linearised systems at a specific operating point but not for large-signal analysis.

Consequently, the dataset must be constructed in such a way that the ANN can model not only the steady-state and the small-signal behavior at a specific operating point but also the dynamic response during transitions between different operating points, even changing the operating mode.

In order to fulfil the above specifications, the input signals are randomly chosen over the entire operating range. The system is excited by giving step waves as input signals to explore the entire frequency spectrum.

B. Design of the NARX-ANN

Two independently variable model are used as inputs: the duty cycle δ and the output current i_o. While the output variables are the inductor current i_L and the output voltage v_o.

The duty cycle is used as control variable and, in the small-signal analysis, it allows to plot the transfer function between the duty cycle and the output voltage G_{δ,v_o}. The output current is used as an input since it permits to verify the effectiveness of the NARX model during rapid load transients. The inputs and the outputs of the model are noted as follows:

$$u(k) = \begin{bmatrix} \delta(k) \\ i_o(k) \end{bmatrix} \qquad \hat{y}(k) = \begin{bmatrix} \hat{i}_L(k) \\ \hat{v}_o(k) \end{bmatrix} \tag{3}$$

A first evaluation of the validity of the proposed solution is carried out using simulative results. The model of the boost converter, shown in Fig. 2, is implemented in the Matlab& Simulink environment and the dataset is collected.

Since the paper aims to develop the average model of a boost converter, the waveforms are passed to a moving average filter with a cut-off frequency that depends on the power converter bandwidth. In this example, a sampling frequency of $10\,\mathrm{kHz}$ is chosen.

The number of operating points uses to train the network depends on the problem at hand and the accuracy required. In this work, a total amount of 75,000 operating conditions (in terms of δ and i_o) are used for the dataset, divided into training (80 %), validation (10%), and testing (10%). To cover the whole workspace during the training phase, the samples of the input signals are randomly chosen over the whole operating range. Each operating point is applied for a fixed time depending on the dynamics of the system. In this work, the δ and i_o operating points are changed at the same time instant and are applied for $2\,\mathrm{ms}$.

The complexity of an NARX-ANN, in addition to the number of layers and neurons, in the case of NARX-ANN, is also given by the number of delays associated with the inputs and outputs. Since the ANN is used to replicate the average model of a converter, the minimum number of delays required by the network can be set *a-priori*. In this test-case the input signals are delayed of one step while, the output signals, are two steps delayed. Additional tests are carried out to verify the operation of the network with a greater number of delays, but no significant improvements are recorded.

The inputs of the NARX-ANN are:

$$\begin{aligned} u(k) = \quad & [\delta(k), i_o(k), \delta(k-1), i_o(k-1), i_L(k-1), \\ & v_o(k-1), i_L(k-2), v_o(k-2)] \end{aligned} \tag{4}$$

and they are normalised between 0 and 1.

While the outputs are:

$$y(k) = [i_L(k), v_o(k)] \tag{5}$$

Since all the inputs are normalised, the performance of the model does not depend on the range of input variables. Therefore, the same approach could be used to model an

TABLE II: NARX-ANN hyperparameters of simulation test.

Hyperparameter	Value	Hyperparameter	Value
Training size	60,000	nr° of parameters	1527
Validation size	12,500	Optimizer	*Adam*
Test size	12,500	Loss	*mse*
nr° of Neurons in HL_1	40	Learning rate	0.001
nr° of Neurons in HL_2	20	Epochs	1598
nr° of Neurons in HL_3	15	Training time	5400 s

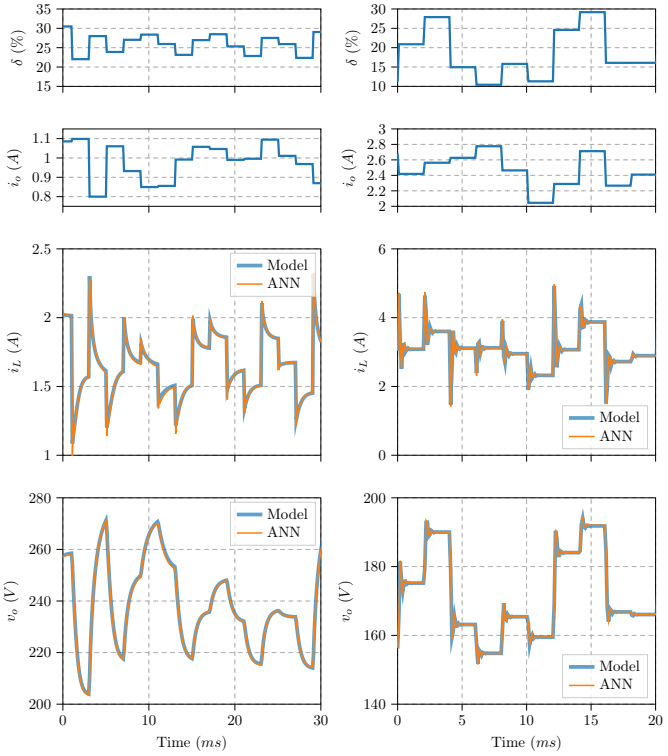

(a) DCM operating mode (b) CCM operating mode

Fig. 3: Comparison between model outputs and those predicted by the neural network. In (a-b) the i_L and v_o waveforms in DCM while in (c-d) in CCM.

equivalent boost converter with an higher input and output values.

The NARX-ANN is developed using the library Tensorflow 2.8 on Python and the training phase is carried out in a NVIDIA GeForce RTX 3070 Ti.

The hyperparameters of the NARX-ANN (Tab. II) are chosen using a manual research algorithm and they are a trade-off between accuracy and the amount of time required for the training.

C. Simulation results

The NARX-ANN is first evaluated in the time domain. To visualize the performance of the model, the RMSE is computed on the test-set obtaining an error of 23 mA for the current and 271 mV for the voltage.

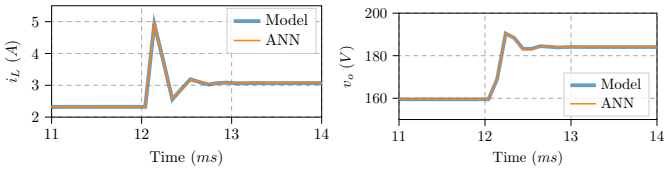

(a) Inductor current i_L (b) Output voltage v_o

Fig. 4: Transition of the i_L and v_o between two operating point in CCM operation.

Furthermore, in order to demonstrate how the ANN can estimate the behavior of the boost converter in both DCM and CCM operation, a small set of operating points in DCM and CCM are chosen from the test-set and the performances are evaluated in Fig. 3(a) for DCM operation and in Fig. 3(b) for CCM operation.

As depicted in Fig. 3, ANN is able to accurately estimate both the inductor current i_L and the output voltage v_o in both converter operating modes, even during transition between two working points (Fig. 4).

To show how a NARX-ANN model can be used for small-signal analysis of a EPC, a transfer function for each operating mode is shown in Fig. 5. The transfer functions are obtained over a total of 20 points between 3 Hz and the Nyquist frequency of 5 kHz (dotted lines in Fig. 5).

In general, the small-signal analysis obtained by NARX-ANN show good correlation with the model-derived analysis with an error that increases as the Nyquist frequency is approached.

NARX-ANN also presents similar results for other working points that have not been reported in Fig. 5.

IV. Experimental Setup

To verify the performance of the proposed approach using real data, the prototype of Fig. 6 is used. The converter has the same parameters of the simulation one and they are reported in Tab. I.

The output current source in Fig. 2 is replaced with a current-controlled load. It consists of a half-bridge converter switching at 50 kHz with an active load in a constant-voltage mode connected in parallel V_l equals to 380 V. The output current reference i_o is achieved via a current control loop consisting of a proportional-integral regulator. In this case each operating point is applied for 10 ms in order to allow the regulator to adjust the output current.

Both power converters are implemented in an in-house rapid prototyping system using Imperix modules.

As depicted in Fig. 6(a), four variables are acquired using the CompactRio FPGA environment provided by National Instrument with a sampling frequency of 10 kHz. The sampling variables are filtered inside the in-house rapid prototyping system using a finite impulse response filter with a cut-off frequency equal to the sampling one.

The characteristics with which the experimental dataset is acquired are the same as those used for the design of the

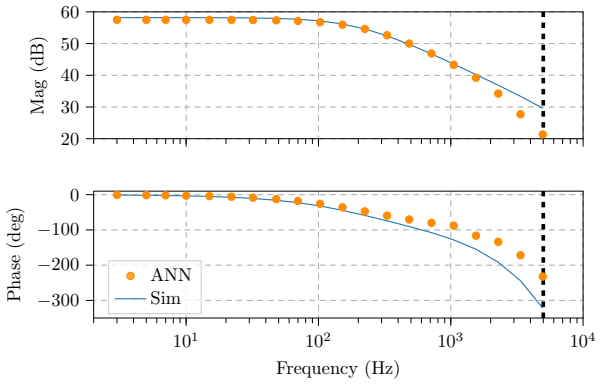

(a)

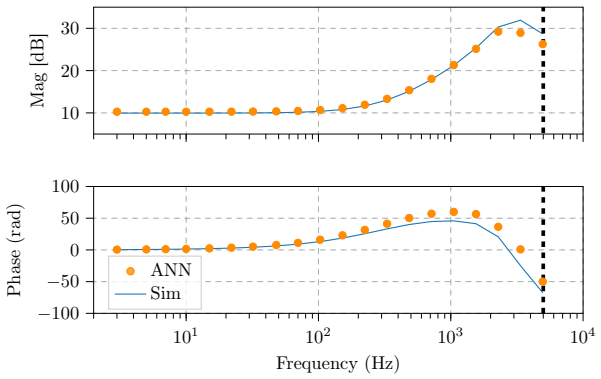

(b)

Fig. 5: Comparison of frequency responses between simulation model and ANN for different operating points. (a) DCM: G_{δ,v_0} with δ=30% and i_o=1 A (b) CCM: G_{δ,i_L} with δ=20% and i_o=2 A. The black dotted lines denotes the Nyquist frequency.

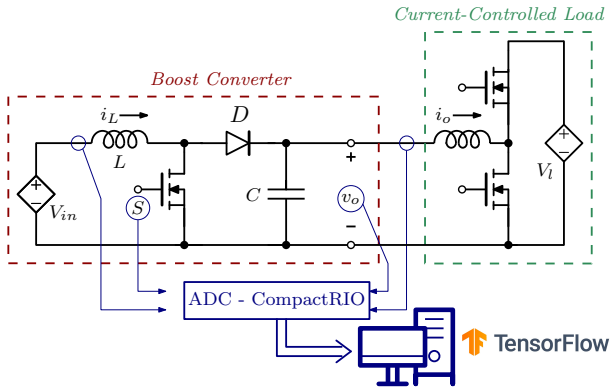

(a)

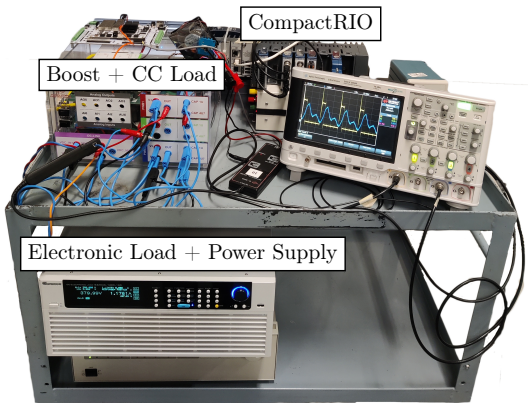

(b)

Fig. 6: In (a) the schematic of the boost converter and the current-controlled current source and in (b) the experimental setup.

simulative one. Therefore a total amount of 75,000 operating conditions are acquired to cover the whole workspace.

The hyperparameters of the ANN are the same as those used for the experimental part shown in Tab. II. In this case the time required by the training phase is 8500 s for a number of epochs equal to 3201. The time required is longer than in simulation because each operating point is applied for a longer period.

The final error on the experimental test-set is 74 mA for the current and 980 mV for the voltage

V. Experimental Results

This section shows how the model developed using NARX-ANN can be used to predict the system response in DCM and CCM, in time or frequency domains using experimental data.

In Fig. **??** the response of the NARX-ANN, trained with the experimental dataset, is evaluated versus the true output of the system. While Fig. 8 shows a zoom-in of Fig. **??** during the change of working point for current i_l and voltage v_o in CCM operating mode.

As for the simulation tests, the comparison between the model frequency response and the one obtained using the ANN model is drawing e the transfer functions are plotted in Fig. 9).

Although there is more noise in the experimental measurements, the same conclusions can be drawn as in the simulation test.

VI. Conclusion

An approach based on the application of NARX-ANN for modeling non-linearities in power converters is presented. In addition, several considerations have been made regarding the criteria with which the dataset is designed. The validity of the proposed model is verified in both time and frequency domains by using and experimental measurements carried out considering a boost converter as test-case. The experimental results shown good matching in time and frequency domains for both the operating modes of the converter even during the transition between different working points. The proposed method is considered as a first step in black-box modeling of converters non-linearities using AI techniques.

References

[1] S. Zhao *et al.*, "An Overview of Artificial Intelligence Applications for Power Electronics," *IEEE Transactions on Power Electronics*, vol. 36, no. 4, pp. 4633–4658, 2020.

[2] V. Valdivia *et al.*, "Black-box modeling of three-phase voltage source inverters for system-level analysis," *IEEE Transactions on Industrial Electronics*, vol. 59, no. 9, pp. 3648–3662, 2011.

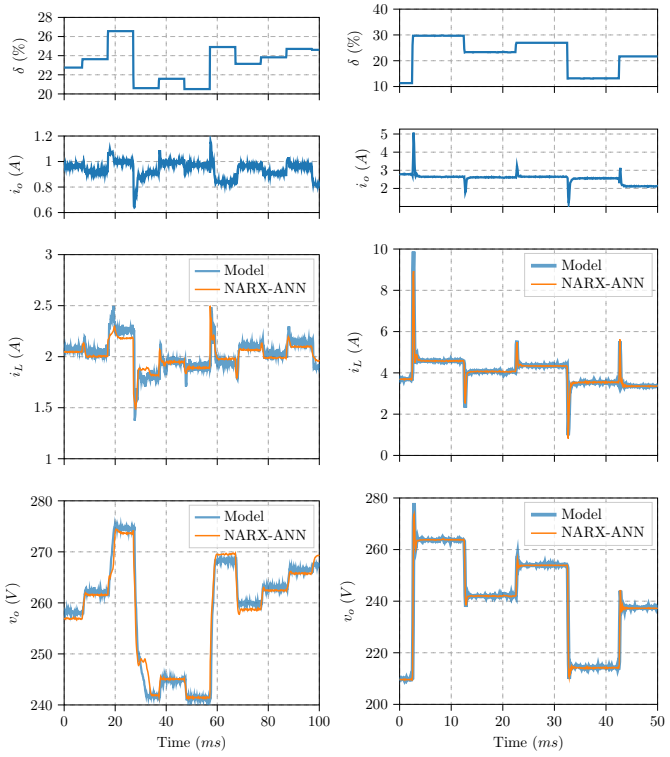

(a) DCM opereting mode (b) CCM operating mode

Fig. 7: Comparison between model outputs and those predicted by the neural network. In (a-b) the i_L and V_o waveforms in DCM while in (c-d) in CCM.

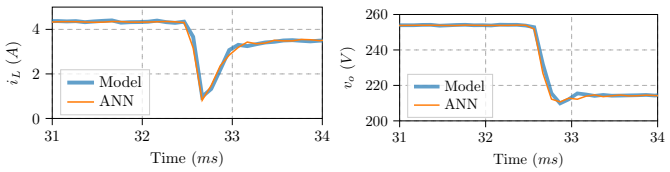

(a) Inductor current i_L (b) Output voltage v_o

Fig. 8: Transition of the i_L and v_o between two operating point in CCM operation using experimental data.

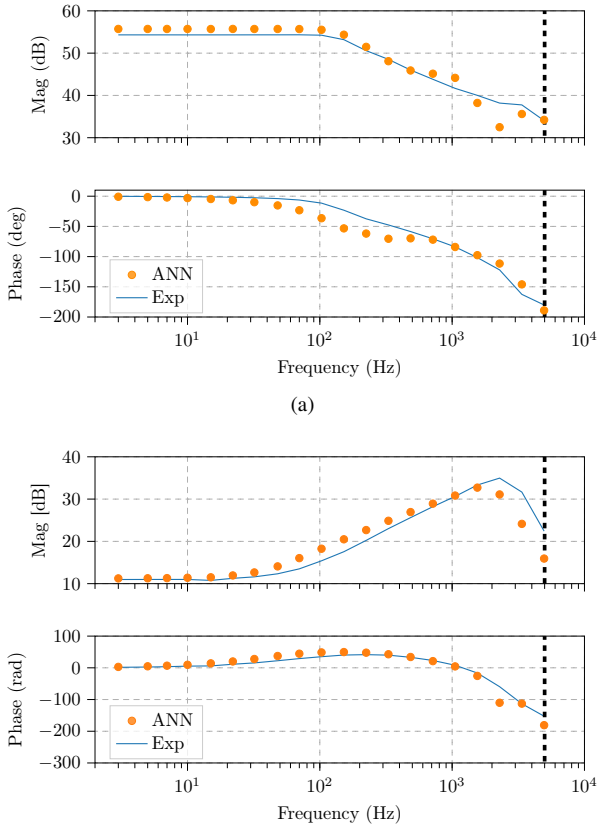

(a)

(b)

Fig. 9: Comparison of frequency responses between experimental modeling and ANN for different operating points. (a) DCM: G_{δ,v_0} with δ=30% and i_o=1 A (b) CCM: G_{δ,i_L} with δ=20% and i_o=2 A. The black dotted lines denotes the Nyquist frequency.

[3] ——, "Simple Modeling and Identification Procedures for "Black-Box" Behavioral Modeling of Power Converters Based on Transient Response Analysis," *IEEE Transactions on Power Electronics*, vol. 24, no. 12, pp. 2776–2790, 2009.

[4] A. Wunderlich *et al.*, "Hybrid analytical and data-driven modeling techniques for digital twin applications," in *2021 IEEE Electric Ship Technologies Symposium (ESTS)*. IEEE, 2021, pp. 1–7.

[5] A. Frances *et al.*, "Blackbox Polytopic Model with Dynamic Weighting Functions for DC-DC Converters," *IEEE Access*, vol. 7, pp. 160 263–160 273, 2019.

[6] G. Ala *et al.*, "A Local Linear Black-Box Identification Technique for Power Converters Modeling," in *2009 IEEE Vehicle Power and Propulsion Conference*. IEEE, 2009, pp. 257–264.

[7] I. Cvetkovic *et al.*, "Non-linear, Hybrid Terminal Behavioral Modeling of a DC-based Nanogrid System," in *2011 Twenty-Sixth Annual IEEE Applied Power Electronics Conference and Exposition (APEC)*. IEEE, 2011, pp. 1251–1258.

[8] J. A. Oliver *et al.*, "Hybrid Wiener-Hammerstein Structure for Grey-Box Modeling of DC-DC Converters," in *2009 Twenty-Fourth Annual IEEE Applied Power Electronics Conference and Exposition*, 2009, pp. 280–285.

[9] A. Francés *et al.*, "The Performance of Polytopic Models in Smart DC Microgrids," in *2016 IEEE Energy Conversion Congress and Exposition (ECCE)*, 2016, pp. 1–8.

[10] A. Wunderlich and E. Santi, "Digital Twin Models of Power Electronic Converters Using Dynamic Neural Networks," in *2021 IEEE Applied Power Electronics Conference and Exposition (APEC)*. IEEE, 2021, pp. 2369–2376.

[11] G. Rojas-Dueñas *et al.*, "Black-Box Modelling of a DC-DC Buck Converter Based on a Recurrent Neural Network," in *2020 IEEE International Conference on Industrial Technology (ICIT)*. IEEE, 2020, pp. 456–461.

[12] P. Qashqai *et al.*, "Modeling Power Electronic Converters Using A Method Based on Long-Short Term Memory (LSTM) Networks," in *IECON 2020 The 46th Annual Conference of the IEEE Industrial Electronics Society*. IEEE, 2020, pp. 4697–4702.

[13] G. Rojas-Dueñas *et al.*, "A Deep Learning-Based Modeling of a 270 V-to-28 V DC-DC Converter Used in More Electric Aircrafts," *IEEE Transactions on Power Electronics*, vol. 37, no. 1, pp. 509–518, 2021.

[14] S.-C. Wang, "Artificial Neural Network," in *Interdisciplinary computing in java programming*. Springer, 2003, pp. 81–100.

[15] H. Hewamalage *et al.*, "Recurrent Neural Networks for Time Series Forecasting: Current status and future directions," *International Journal of Forecasting*, vol. 37, no. 1, pp. 388–427, 2021.

[16] Z. Boussaada *et al.*, "A Nonlinear Autoregressive Exogenous (NARX)

Neural Network Model for the Prediction of the Daily Direct Solar Radiation," *Energies*, vol. 11, no. 3, p. 620, 2018.
[17] P. G. Benardos and G.-C. Vosniakos, "Optimizing Feedforward Artificial Neural Network Architecture," *Engineering applications of artificial intelligence*, vol. 20, pp. 365–382, 2007.
[18] S. Sharma *et al.*, "Activation Functions in Neural Networks," *Inter. Jour. of Eng. Appl. Sciences & Tech.*, vol. 4, pp. 310–316, 2020. [Online]. Available: http://www.ijeast.com
[19] R. W. Erickson and D. Maksimovic, *Fundamentals of Power Electronics, 3rd edition*. Springer, 2020.
[20] R. D. Middlebrook, "Measurement of loop gain in feedback systems," *International Journal of Electronics Theoretical and Experimental*, vol. 38, no. 4, pp. 485–512, 1975.
[21] B. Miao *et al.*, "System Identification of Power Converters with Digital Control Through Cross-Correlation Methods," *IEEE Transactions on Power Electronics*, vol. 20, no. 5, pp. 1093–1099, 2005.
[22] A. Fernández-Herrero *et al.*, "Use of multisine excitations for frequency-response measurement of nonlinear dc-dc switching converters," in *2012 Twenty-Seventh Annual IEEE Applied Power Electronics Conference and Exposition (APEC)*. IEEE, 2012, pp. 735–739.